Conductor Performance Qualification of TFKO3 Sample for ITER TF Magnet

Soo-Hyeon Park, Soun Pil Kwon, Keeman Kim, Boris Stepanov, and Pierluigi Bruzzone

***Abstract*—Two identical conductor samples were fabricated from 110 m length cable prepared for qualification of the manufacturing process for Phase II procurement of ITER TF conductor. Superconducting strand characteristics, cabling specifications, and the stainless steel jacket sections are described. Sample assembly and instrumentation of various voltage taps and temperature sensors have been prepared according to specified procedures for conductor performance qualification. The performance test program which was agreed to by the SULTAN working group was applied to the conductor samples. To assess the current sharing temperature (T_{cs}), standard analysis procedures were adopted. The T_{cs} of both samples at 68 kA with a background field of 10.78 T after a 1000 cyclic load are well above the acceptance criteria. Behavior of individual "star" voltage taps which are located at different positions and which are possible origins of rather large discrepancies in the T_{cs} of identical samples is discussed. The effective strain and the transition index of the samples are obtained from the experimental data.**

***Index Terms*—ITER, Nb_3Sn strand, SULTAN, TF conductor.**

I. Introduction

After the successful results of TFKO2 conductor samples tested in SULTAN [1], the Korean Domestic Agency (KODA) for the ITER project began mass production of the ITER TF conductor. Up to now, Kiswire Advanced Technology (KAT) has produced 35 tons of Nb_3Sn strand using the internal tin route, Nexans Korea manufactured nine cables including two for qualification, and POSCO Specialty Steel (POSCOSS) fabricated 2 km of tubes for jacketing.

As a prerequisite for the production of conductors to be used in the ITER tokamak machine, the Procurement Arrangement requires process qualification, whose scope is the manufacturing and characterization of one Cu dummy conductor and one 100 m length superconducting conductor for every strand/cable/jacket combination [2]. One of the final acceptance tests for process qualification is the full size Conductor Performance Qualification Sample (CPQS) test at the SULTAN facility at CRPP (Centre de Recherches en Physique des Plasmas) which is the subject of this article.

Manuscript received September 09, 2011; accepted November 26, 2011. Date of publication December 05, 2011; date of current version May 24, 2012. This work was supported by the Ministry of Education, Science and Technology of Korea and the Ministry of Knowledge Economy of Republic of Korea under Contract of the ITER Korea Project (2009-0081593).

S.-H. Park, S. P. Kwon, and K. Kim are with National Fusion Research Institute, Daejeon 305-333, Republic of Korea (e-mail: shpark@nfri.re.kr).

B. Stepanov and P. Bruzzone are with CRPP (Centre de Recherches en Physique des Plasmas), Fusion Technology, CH-5232 Villigen PSI, Switzerland (e-mail: boris.stepanov@psi.ch; pierluigi.bruzzone@psi.ch).

Color versions of one or more of the figures in this paper are available online at http://ieeexplore.ieee.org.

Digital Object Identifier 10.1109/TASC.2011.2178109

TABLE I
Summary of Strand Performance Parameters

Billet 01KK	Occ.	I_c (A)	J_c (A/mm^2)	RRR	Q_h (mJ/cm^3)	Cu/Non Cu ratio	Dia. (mm)
3	56	284.9	1040	130	306	0.93	0.821
5	48	266.7	1042	117	500	1.07	0.821
8	67	280.0	1012	138	390	0.92	0.822
9	75	271.3	1008	147	382	0.96	0.820
10	54	263.0	961	147	341	0.93	0.820
11	67	290.5	1050	134	326	0.91	0.819
12	65	295.7	1070	129	342	0.91	0.820
13	75	260.7	981	133	346	0.99	0.820
14	56	275.7	997	157	383	0.91	0.821
15	77	269.5	1000	178	360	0.96	0.820
16	70	267.5	964	115	440	0.90	0.820
17	66	290.0	1049	154	423	0.91	0.819
18	56	276.3	998	159	519	0.90	0.820
19	68	294.5	1111	154	514	0.99	0.820
CABLE	900	277.6	1020	142	398	0.94	0.820

Two conductor samples named TFKO3 were prepared from a 118 m length cable. Samples were heat treated and assembled at CRPP. A standard test procedure [3] agreed to among the ITER Organization (IO), DAs, and CRPP was strictly applied to the test, and the current sharing temperature, T_{cs}, was assessed in accordance with a standard analysis procedure [4]. In this article, we present the details involved in sample preparation and the test results.

II. TFKO3 Sample Preparation

A. Nb_3Sn Strand

14 restacking billets were used for the 118 m length cable. The strand design is the same as that of the right leg of TFKO2, and details are described elsewhere [1].

Table I summarizes major performance parameters and the occurrence number of strand billets in the cable.

All billet IDs start with "01KK" and end with a four digit number, for example, 01KK0016. Occ. is the number of occurrences of the strand billet in the conductor. The critical current (I_c) is measured at 4.2 K with an external field of 12 T. Non-Cu critical current density (J_c) is a derived quantity which is calculated using I_c, the Cu/non Cu ratio, and the strand diameter. RRR is the ratio of electrical resistivity at 273 K to that at 20 K. Hysteresis loss (Q_h) is the integrated area of the magnetization curve versus magnetic field between ± 3 T.

Since strands in the conductor experience severe loads due to thermal contraction and electromagnetic force, understanding of the functional dependence of the critical current on strain is very important. In order to determine the scaling relation, measurements of the critical current as a function of magnetic field, temperature, and strain were performed on strand 01KK0016. The detailed experimental method is described in [5].

TABLE II
SCALING PARAMETERS OF 01KK0016

C	B_{c20m} (T)	T_{c0m} (K)	C_{a1}	C_{a2}	$e_{0,a}$ (%)	p	q
35986	31.58	15.95	70.28	32.91	0.44	0.83	2.49

TABLE III
SPECIFICATIONS AND RESULTS OF INSPECTION OF THE CABLE

Verification item	Specification	Result
Cable Pattern	((2sc+1Cu)x3x5x5+core)x6	PASS
Core	3x4	PASS
Outer Diameter	40.5+0.2-0.3 mm	40.5 mm
Cable wrap		
- thickness	0.10±0.01 mm	0.10 mm
- width	40±2 mm	40.0 mm
- overlapping	40+0-10 %	39 %
Cable twist pitch	420±20 mm	440 mm
Sub-cable wrap		
- thickness	0.10±0.01 mm	0.10 mm
- width	15±2 mm	15 mm
- surface cover	50±5 %	47 % ~ 52 %
Twist pitch (stage 4)	300±15 mm	310 mm
Twist pitch (stage 3)	190±10 mm	185 mm
Twist pitch (stage 2)	140±10 mm	145 mm
Twist pitch (stage 1)	80±15 mm	80 mm
Copper core Twist pitch (stage 2)	140±10 mm	140 mm
Copper core Twist pitch (stage 3)	80±5 mm	80 mm

Table II shows parameters which best fit the experimental data to a model proposed by the IO [6].

B. Cable Specification

Cable for ITER TF coils is manufactured in five stages mixing Nb_3Sn-based and Cu strands and incorporates a stainless steel cooling spiral at its core during the last stage of cabling [2]. The fourth-stage sub cables and the final cable are wrapped with stainless strips that provide mechanical protection and limit inter-strand coupling currents.

Nexans Korea performed the cabling with tubular machines for the first three stages, and a planetary machine for the fourth and fifth stages. The 118 m length cable was manufactured, and destructive inspection of two 1 m length samples one from the point and the other from the tail of the cable was performed. The cable specifications and results from the inspection of the point sample are shown in Table III.

C. Jacket Section and Jacketing

A 10 m length section from the 118 m long cable was cut for jacketing. A stainless steel tube made by POSCOSS was used as a jacket section. Length, outer diameter and thickness of the tube are 8.0 m, 48.0 mm, and 1.9 mm respectively. Techniques to characterize the tube including the low temperature tensile test are described in [7], [8]. The cable section inserted in the tube was drawn through a compaction roller to a diameter of 43.7 mm. The estimated void fraction of the jacketed conductor was 29%. The conductor was then divided into two 4 m length conductor sections and shipped to CRPP where the heat treatment, sample assembly and instrumentation were performed.

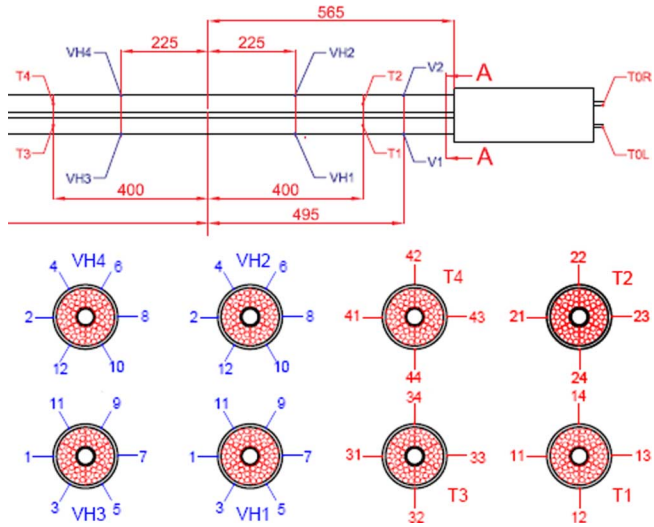

Fig. 1. Instrumentation of the TFKO3 sample. Lower conductor is the *left leg*, and the upper conductor is the *right leg*. The distance between voltage taps is 0.45 m. The lower diagram illustrates the location of voltage taps and temperature sensors as viewed from the top of the samples in SULTAN.

D. Heat Treatment, Sample Assembly and Instrumentation

The two conductor sections were cut to the exact length of 3419 mm, and the jacket was dismantled from both ends of the two sections for joint fabrication. The conductor terminations were prepared by compacting a prefabricated copper sleeve with EB welded steel caps onto the cable after removing the Cr plating. To prevent any slippage between jacket and cable two crimping rings were crimped onto the conductor at both ends, 29 mm away from the jacket edge.

The heat treatment of the TFKO3 conductors was carried out in a tube furnace in vacuum, with a residual pressure smaller than $3.8 \cdot 10^{-6}$ mbar. During the entire treatment a flow of high-purity argon (≈0.2 liter/min) purged the sample of any gases or fumes. The heat treatment schedule was 50 hours at 210°C, 25 hours at 340°C, 25 hours at 450°C, 100 hours at 575°C, 120 hours at 650°C, and then a gradual cool down to room temperature. The temperature ramp rate was kept at 5°C/h.

Two legs were assembled and an array of voltage taps and temperature sensors were attached. Joints and terminals were fabricated according to a solder filled procedure [9], which allows independent control of the helium inlet temperature in each of the two legs. Fig. 1 shows a schematic of the instrumentation. VHij is a notation for voltage taps where i denotes the longitudinal locations in both legs and j specifies the angular positions in the crown arrays.

III. TEST RESULTS AND ANALYSES

The major purpose of the CPQS test at SULTAN is the assessment of the current sharing temperature T_{cs} at a background magnetic field of 10.78 T and an operating current of 68 kA through the samples for the case of ITER TF conductors. A single T_{cs} run consists of ramping up the current step by step, up to the operating current under a constant field of 10.78 T, and then, a ramping up in temperature, also step by step until samples quench. Fig. 2 demonstrates highlights of the T_{cs} run, by displaying current, temperature, and the signal of a selected voltage tap pair (VH11VH31) as a function of time during the

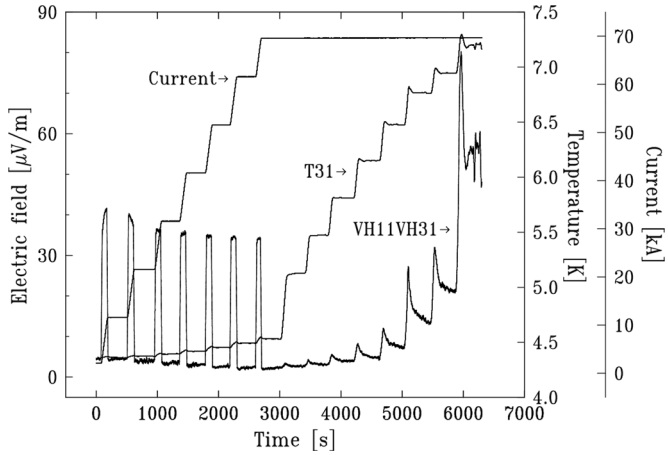

Fig. 2. Voltage (VH11VH31), temperature (T31), and current during a T_{cs} run at the first cycle ($N = 1$). Electric field is obtained from the voltage divide by the distance between voltage taps, 0.45 m. All the signals were centered averaged for 501 data points.

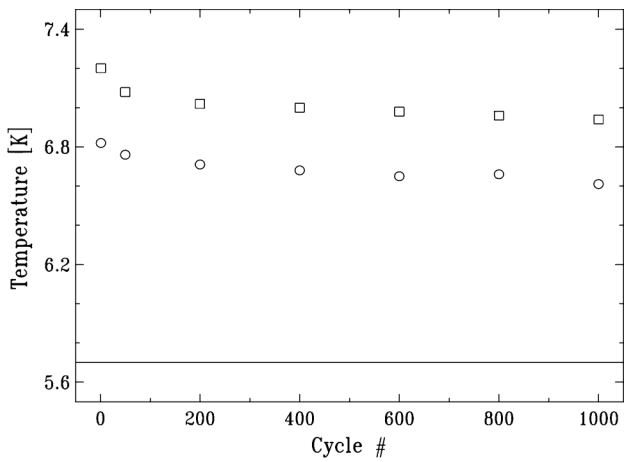

Fig. 3. Evolution of T_{cs} up to the cycle 1000. Circles and squares represent the T_{cs} of the left and right legs respectively. The acceptance criteria, which is 5.7 K is shown with a solid line.

TABLE IV
EVOLUTION OF THE T_{cs}

Cycle #	1	50	200	400	600	800	1000
T_{cs} (left) (K)	6.82	6.76	6.71	6.68	6.65	6.66	6.61
T_{cs} (right) (K)	7.20	7.08	7.02	7.00	6.98	6.96	6.94

first cycle ($N = 1$). Samples were driven with currents going from 0 to 68 kA repeatedly, and at specified cycles ($N = 50$, 200, 400, 600, 800, and 1000), a T_{cs} run was performed.

The *early voltages* and/or the *voltage slopes* [9] are small enough to ignore the *linear correction* described in [4]. The offsets of all voltage tap arrays of each leg were within 1 μV at 68 kA. Terminations and joint resistances were 0.47 nΩ for the left leg, 0.51 nΩ for the right leg, and 0.40 nΩ for the joint before cyclic loading.

T_{cs} was assessed in accordance with a standard procedure [3], [4]. Evolution of the T_{cs} of both legs during a cycle is shown in Fig. 3. The T_{cs} of both legs were well above the acceptance criteria set by the IO which is 5.7 K after 1000 cycling. Table IV summarizes the evolution of the T_{cs}.

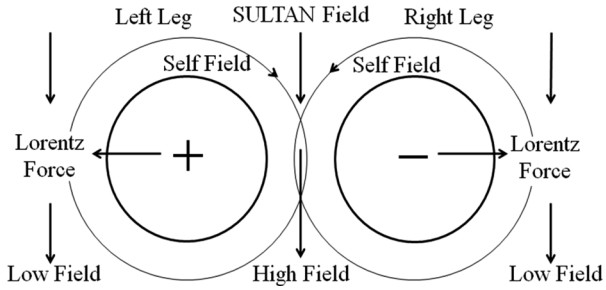

Fig. 4. Top view of the magnetic field configuration. A combination of the background field and the self field produces the field gradients.

TABLE V
T_{cs} OF INDIVIDUAL VOLTAGE TAPS AT $N = 1$

T_{cs} (v1)	T_{cs} (v3)	T_{cs} (v5)	T_{cs} (v7)	T_{cs} (v9)	T_{cs} (v11)	T_{cs} (avg)
6.84	6.78	6.70	6.86	6.87	6.88	6.82
T_{cs} (v2)	T_{cs} (v4)	T_{cs} (v6)	T_{cs} (v8)	T_{cs} (v10)	T_{cs} (v12)	T_{cs} (avg)
7.22	7.12	7.14	7.25	7.25	7.25	7.21

The *star* voltage taps enable one to evaluate the T_{cs} by individual voltage tap. Since the magnetic field across the conductor section is not homogenous due to the self field, and the Lorentz force has a definite direction (See Fig. 4), locations of the voltage taps could be clearly grouped as the *high field part* (HFP) and the *low field part* (LFP). For the left leg, VH19VH39 (v9), VH111VH311 (v11) are in the HFP and VH13VH33 (v3), VH15VH35 (v5) are in the LFP. It should be noted that this field inhomogeneity refers to the cross section field due to the self field, and it is distinguished from the high/low field zone due to the longitudinal background field gradient of SULTAN. The remaining two sets, v1 and v7 are in the neutral part. With the same notation, v4, v6 are in the LFP, v10, v12 are in the HFP, and v2, v8 are in the neutral part for the right leg.

T_{cs} values were derived from the individual voltage taps at the first cycle and results are shown in Table V. Temperatures were assumed to be uniform and were calculated by averaging the values of 8 temperature sensors. One can clearly figure out that the T_{cs} of both legs are lower in the LFP. Furthermore, this feature persisted for every cycle up to $N = 1000$.

The *cabling effect* is considered to play a role in smearing out any differences between petals, including the Lorentz force. In addition, the distance between voltage taps (450 mm) is very close to the nominal twist pitch of the cable (440 mm). At this stage, it is not clear whether the different behaviors of the individual voltage taps are caused by the slight mismatch in the two lengths. At least, our results could be another justification for the adoption of star voltage taps.

The effective strain and the transition index (n value) of the conductor can be obtained from a method described in the standard procedure [4]. In this method, the electric field of a conductor is approximated as

$$E(T) = \frac{E_0}{LA} \iint_{LA} \left[\frac{J_{op}}{J_c(B, T, \varepsilon_{eff})} \right]^n dA dz \qquad (1)$$

Where A is the cable area, L is the distance between the voltage taps (=0.45 m), E_0 is 10 μV/m, and J_{op} is the current of

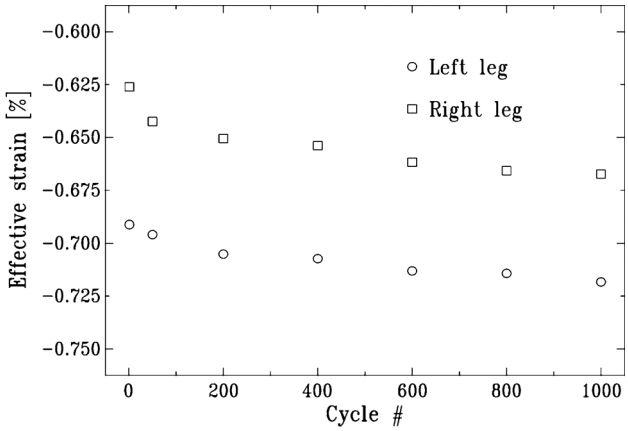

Fig. 5. Evolution of the effective strain of the left and right legs.

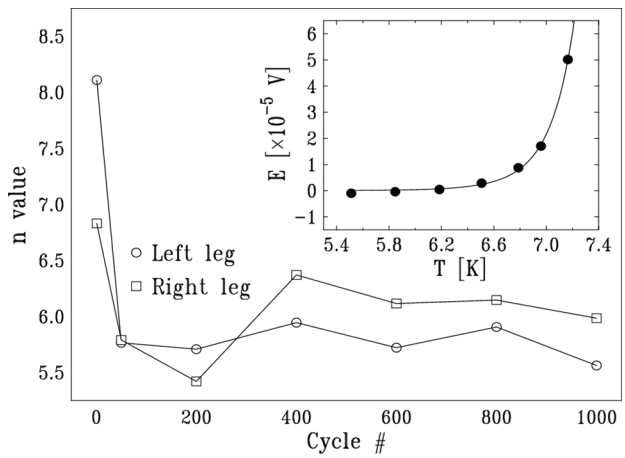

Fig. 6. Evolution of the n value of the left and right legs. Connecting lines are for guidance only. The inset shows the electric field of the left leg versus temperature at $\mathrm{N} = 1$. The curve in the inset is the fitted result of the electric field to (1).

the non-copper area. The magnetic field is assumed to be linearly varying across the cable area due to the self field. The $J_c(B, T, \varepsilon_{eff})$ scaling relation described in Section II is required for the analysis. Figs. 5 and 6 show the evolution of the effective strain and the n values of both legs determined by the best fit of the above $E(T)$ curve to the data points in the $\mathrm{T_{cs}}$ runs.

TFKO3 is a conductor made from multiple billets. In such a case, the integrand of (1) should be replaced with the occurrence weighted summation on the billets, and the scaling parameters of all billets should be known. Instead, we have taken an approximation that the scaling characteristics of the 14 billets in Table I are very similar to those of 01KK0016, and the summation could be represented as a single virtual billet. The distribution of J_c was embodied by applying the overall scaling strength (C in Table II) as the fitting parameter of (1).

Equation (1) bears an important assumption that the current and the strain are uniform in the conductor. Therefore, one should be very careful to interpret the analysis. Recent work [10] reveals that the effective stain in Cable-In-Conduit Conductors (CICC) could be regarded as a combination of the axial strain and the bending strain, and has a bell shape distribution. From this point of view, the effective strain in (1) can be attributed to the mean value over the distribution.

A final remark should be made on the rather large discrepancy of $\mathrm{T_{cs}}$ ($\sim$0.3 K) between the two legs. It is a surprising result because both legs are fabricated using the same procedure and strands from the same billets. If we exclude the possibility that there were any differences in the heat treatment and instrumentation, the gradual change of the twist pitches of the conductors might be a cause of the difference. However, it is hard to believe that such a large discrepancy could be explained by differences in the twist pitches. At this moment, we have no reasonable explanation for the result, and causes of the significant difference in the $\mathrm{T_{cs}}$ are under investigation.

IV. Summary and Conclusion

Two Korean ITER TF conductor samples were fabricated and tested at SULTAN. The $\mathrm{T_{cs}}$ assessment has been performed in accordance with standard procedure, and the results are well above the acceptance criteria. Behaviors of individual voltage taps are discussed. The effective strain and the transition index during cyclic loads are also analysed.

References

[1] D. K. Oh, S.-H. Park, K. Kim, and P. Bruzzone, "Performance test of TFKO2 qualification sample of ITER TF Conductor," *IEEE Trans. Appl. Supercond.*, vol. 20, no. 3, pp. 458–461, Jun. 2010.

[2] Procurement Arrangement 1.1.P6A.KO.01.0 ITER Organization, 2008, Annex B, p. 59.

[3] D. Bessette, Procedure for ITER/TF SULTAN Tests unpublished [Online]. Available: https://user.iter.org/?uid=2N2WBU

[4] D. Bessette, Procedure for $\mathrm{T_{cs}}$ Assessments of the ITER/TF SULTAN Samples unpublished [Online]. Available: https://user.iter.org/?uid=2NPGQ9

[5] S. Oh, C. Lee, H. Choi, K. Moon, K. Kim, J. Kim, and P.-Y. Park, "A variable temperature Walters spiral probe for the critical current measurement of superconducting strands," *IEEE Trans. Appl. Supercond.*, vol. 18, no. 2, pp. 1063–1066, Jun. 2008.

[6] L. Bottura and B. Bordini, "$\mathrm{Jc(B, T, \varepsilon)}$ parameterization for the ITER $\mathrm{Nb_3Sn}$ production," *IEEE Trans. Appl. Supercond.*, vol. 19, no. 3, pp. 1521–1524, Jun. 2009.

[7] S.-H. Park, J. Y. Kim, W. W. Park, H. Choi, Y. J. Ma, S. P. Kwon, K. Kim, S. C. Kang, and D. H. Lee, "The effect of plastic deformation on low temperature mechanical and magnetic properties of Austenite 316LN tube for ITER TF conductor," presented at the MT-22, 2012.

[8] S.-H. Park, J. Y. Kim, W. W. Park, H. Choi, Y. J. Ma, S. P. Kwon, K. Kim, S. C. Kang, and D. H. Lee, "The effect of plastic deformation on low temperature mechanical and magnetic properties of Austenite 316LN tube for ITER TF conductor," *IEEE Trans. Appl. Supercond.*, 2012, submitted for publication.

[9] P. Bruzzone, B. Stepanov, R. Wesche, Y. Ilyin, R. Herzog, M. Calvi, M. Bagnasco, and F. Cau, "Methods, accuracy and reliability of ITER Conductor tests in SULTAN," *IEEE Trans. Appl. Supercond.*, vol. 19, no. 3, pp. 1508–1511, Jun. 2009.

[10] H. Bajas, D Durville, D. Ciazynski, and A. Devred, "Numerical simulation of the mechanical behavior of ITER cable-in-conduit conductors," *IEEE Trans. Appl. Supercond.*, vol. 20, no. 3, pp. 1467–1470, Jun. 2010.